Magnetization pinning in modulated nanowires: from topological protection to the "corkscrew" mechanism

Jose A. Fernández-Roldán, Rafael P. del Real, Cristina Bran, Manuel Vázquez and Oksana Chubykalo-Fesenko*

Supplementary information

S1: Magnetization configurations during the magnetization reversal processes

We present a more detailed analysis of the configurations during the magnetization reversal processes. For a small diameter difference, this happens in one field step so that a dynamical magnetization evolution is presented in Fig. SI1. The vortices are formed with the chirality pattern A-CC-CC-A. The vortices centers also form a helicoidal structure in this case. The dynamics of the magnetization under the switching field has been calculated by integration of the Landau-Lifshitz-Gilbert equation with the damping value 0.1. The calculations were performed starting from the previous stable state of the hysteresis loop in a selected example. The result is presented in Fig. SI1. The reversal starts with the vortex cores reduction, the skyrmion tubes formation and propagation inside the middle narrow segment (Fig. SI1a-c) where the size of the core has been largely reduced. The tube breaks into two tubes by the formation of Bloch points (Fig. SI1d). The Bloch points propagate with different velocities in opposite directions (Fig. SI1d-g). During this propagation, the structures formed by the skyrmion tubes with opposite chiralities at the first left and last right modulation transitions are annihilated simultaneously due to the high concentration of magnetostatic charges in those regions as represented in Fig. SI1e. Simultaneously several new Bloch points are formed and start propagating in opposite directions (Fig. SI1e-g). The effect of different chiralities can be observed in Figs. SI1 (e) and (g): we see that the magnetization reversal is the last to happen in the left and right ends where the vortex chiralities are opposite. The reversal process is retarded there due to topological protection between opposite chiral skyrmion tubes, which is absent in the middle section.

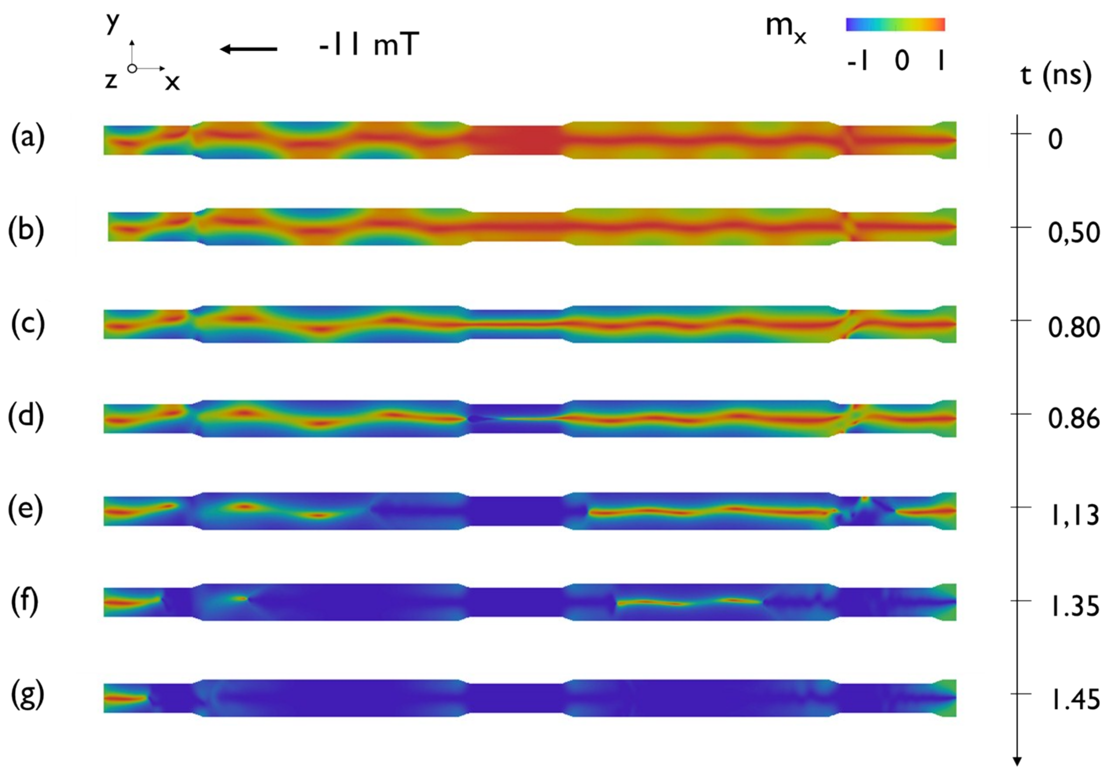

Figure SI1. *(a-g) Longitudinal component of the magnetization in the middle cross section of a nanowire with diameter 100 nm and disorder distribution No.1 at different times during reversal. The nanowire exhibits vortices with chiralities A-CC-CC-A along the nanowire length.*

An example of the reversal process is presented in Fig. SI2 for nanowires with the minor diameter 40 nm and the disorder distribution No.1 (Fig. 1a). The nucleated vortices at the modulation and at the nanowire ends quickly propagate inside the larger modulations and as the field is gradually reduced below zero they become skyrmion tubes. In the left large segment, the vortices have opposite chiralities at the two ends while in the right one show the same chiralities. Consequently, the propagation in the right segment is easy and at H=-170 Oe only one skyrmion tube with a unique chirality is present (See Figure SI2a). In the left wide modulation the vortices at the end of skyrmion tubes with the opposite chirality cannot be easily annihilated and when met, they are divided by a complex domain wall[21] (called a helical domain wall in Ref. 22). Additional field is thus required to annihilate this structure. At H=-180 Oe a small magnetization jump appears in the hysteresis loop (Fig. SI2a), related to a transformation of this wall to a different configuration characterized by a vortex and an antivortex on the surface of the wire (Fig. SI2e). This new structure becomes larger as the field is further increased (See vortex in the inset picture in Figure SI2d). Overall, the narrow segments remain uniformly magnetized until H=-455 Oe when the complete switching takes place in one irreversible jump.

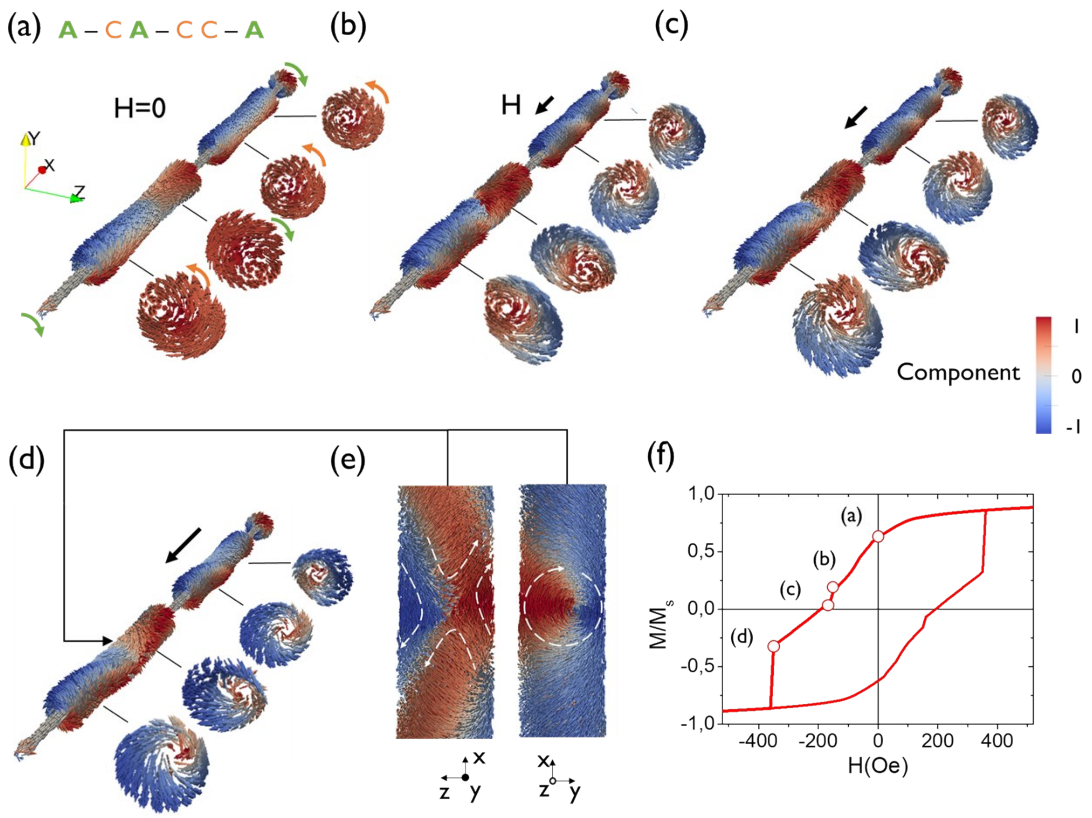

Figure SI2. *Longitudinal component of the surface magnetization of a modulated nanowire with a minor diameter of 40 nm for distribution 2 at different fields marked in the hysteresis cycle (f). (a) remanence, (b) -170 Oe, (c) 180 Oe and (d) and (e) -450 Oe before and after the jump. Inset figures are transverse cross sections of the nanowire at the marked positions in (b-d) where the colors indicate z-component. (e) A cropped perspective of the segment surface longitudinal magnetization at the marked site. Red and blue arrows show the chirality of each vortex/skyrmion. C and A stand for the, Clockwise or Anticlockwise chirality, respectively.*

S2: Analysis of the chirality influence

The magnetization switching in these nanowires takes place by the formation of vortex domains with arbitrary chiralities in the larger segments which should penetrate into the smaller ones. It is clear that there are many possibilities of different chiralities patterns. For small difference in segment diameter we present below the transverse magnetization components and the chirality pattern for the three disorder distributions with hysteresis cycles presented in Fig. 1. One can clearly see the arbitrary chirality pattern which is summarized in Table SI1. The patterns are labelled as X-XX-XX-X, with X, either A or C for Anticlockwise of Clockwise vortex domain chirality, respectively.

	d (nm)	100	80	60	40
Distribution	1	A-CC-CC-C	A-CC-CC-C	A-CC-CC-C	A-CA-CC-A
	2	A-CA-CC-C	A-CA-CC-C	A-CA-CC-C	A-CC-CC-C
	3	A-CA-CA-C	A-AA-CC-A	C-AA-AC-A	A-AA-AA-A

Table SI1. *Chiralities of the vortex structures nucleated at the ends of the wire and at the ends of modulations for each distribution and minor diameter. C (A) indicates the Clockwise (Anticlockwise) chirality following a scheme X-XX-XX-X along the nanowire profile according to Fig. 1.*

By examining the magnetization structures during the hysteresis process in each case we can conclude that in the case of the large difference between the segment diameters, the chiralities of the formed vortex domains have a small effect in the depinning field and the disorder seems to play the crucial role. Consider as an example the disorder distribution corresponding to the case No.3 and d=40nm (Fig. 1c, “strong” pinning) which produced a vortex pattern with the same chirality along the whole nanowire and have the largest depinning field. However, the chiralities of different vortices have a large effect during the propagation stage (which affects the coercive field) resulting (or not) in additional jumps corresponding to the annihilation of vortices of different (or the same) chirality but not on the depinning field itself.

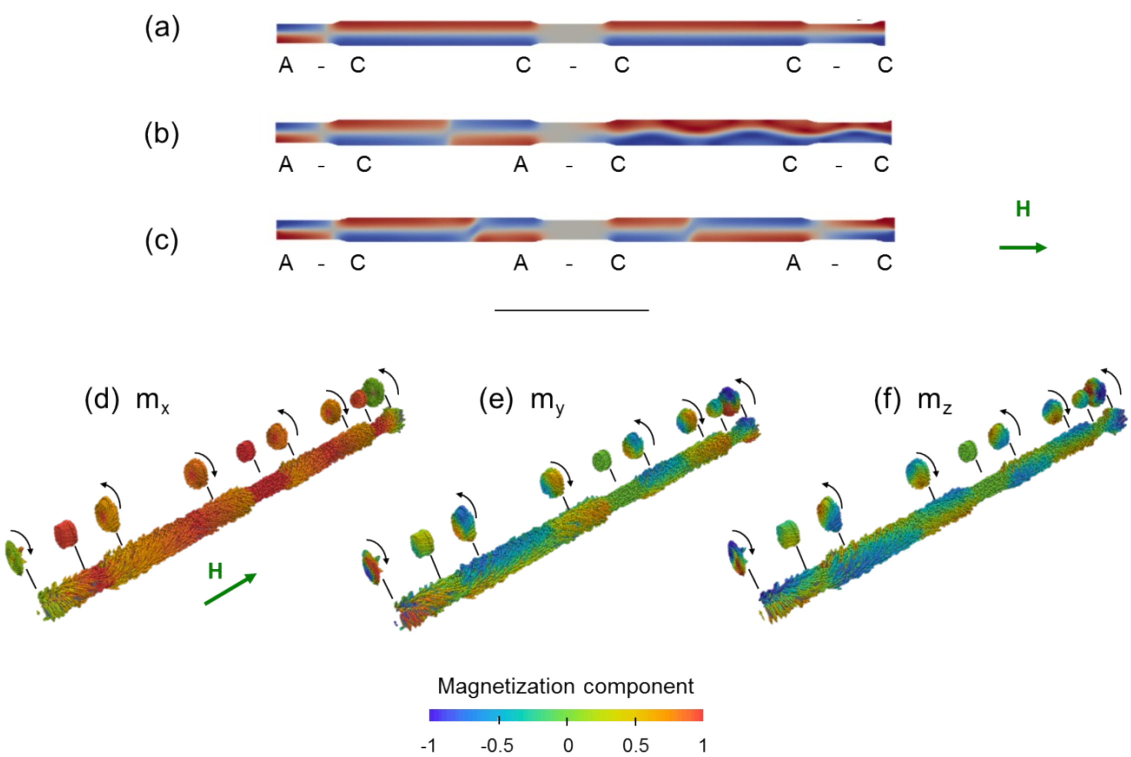

Figure SI3. *(a-c) Schematic representation of the transverse magnetization component inside the nanowires in the middle cross section along the nanowire profile before the switching for d=100 nm for grain distributions with hysteresis cycles of Fig. 1 (m_y>0 red color, m_y<0 blue color and grey color for m_y close to 0). Fig.(a-c) correspond to the grain size distributions* *labelled (1-3) of Fig. 1, respectively. The chirality of each vortex is shown by C(Clockwise) or A (Anticlockwise). (d-f) Surface magnetization distribution corresponding to the nanowire depicted in Fig. SI3(c) showing also the cross-sections with the vortex chiralities.*

The conclusions are different when the difference between the diameters is small ("weak" pinning). In this case the observed chirality pattern plays a major role since the propagation and depinning stage occurs here at the same field. Let us analyze in detail the case with a minor diameter d=100nm. Fig. SI3(a-c) shows schematically the patterns observed for this case. The lowest H_s =-225 Oe corresponds to the nanowire with the distribution 1, for which all vortices have the same diameter and the nanowire nucleates in an almost uniform pattern: clockwise vortices at the ends of all modulations and at the right end of the wire, and a small anticlockwise vortex part on the left end of the wire, see Figure SI3 (a). These domain walls easily propagate along the largest segments and the switching field is minimum. Nevertheless, for disorders 2 and 3, different chiralities are found for the nucleated vortex structures, which lead to different switching fields: H=-255 Oe (for distribution 2) and H=-275 Oe (for distribution 3). When meeting inside a large segment, the vortex domain wall (which have become the skyrmion tubes) with different chiralities produce a complex 180-degree domain wall which requires an extra Zeeman energy for annihilating. The highest switching field value for d=100 nm is obtained for the distribution 3. In this case a completely alternating pattern of vortices with opposite chiralities is produced (Figure SI3 (c)). Note also the helicoidal structure for the vortex domain for the disorder No.2

S3: Analysis of the helicoidal structure

The helicoidal structures presented in Fig. 3(a-b) have been analyzed for the other distributions before the switching field. The results are summarized in Fig SI4 (d-e).

The typical “corkscrew” helicoidal shape for the core positions of the skyrmion tubes is depicted in SI4(a-b) corresponding to different selected diameters. They are characterized by the uniform magnetization at the minor segments and helicoidal tubes connecting them. The effect of the minor diameter variation is the decrease of the amplitude of the helix with d, which are less frequent for d=100nm SI4(c), but not completely absent for every distribution SI4(d). The helix chirality (the handedness of the helix) is found to be arbitrary and the pitch is not uniform along the large segments, becoming larger in the middle of the large segments in the absence of tubes of opposite chiralities. It is also noticed that the minor segments are almost magnetized uniformly for larger diameters which can be seen comparing the last right minor segment for each diameter in Fig SI4(d). The minimization of magnetic charges at the diameter transition regions leads to partial demagnetization of the minor segments. It also makes the skyrmion tubes longer by allowing them to partially penetrate into the minor segments. This reduction of magnetized area in the minor segments due to magnetostatic energy minimization increases the switching field observed in Fig. 1.

As is previously mentioned, the effect of the opposite chiralities of two consequent vortices is to create a topologically protected structure which may be present for every diameter even without the corkscrew shape. These structures are seen in Figs. SI4(b, c). This effect is even stronger for minor diameters and leads to the high switching fields in Fig. 1 as a consequence of the confinement of the skyrmion tubes inside the minor segments.

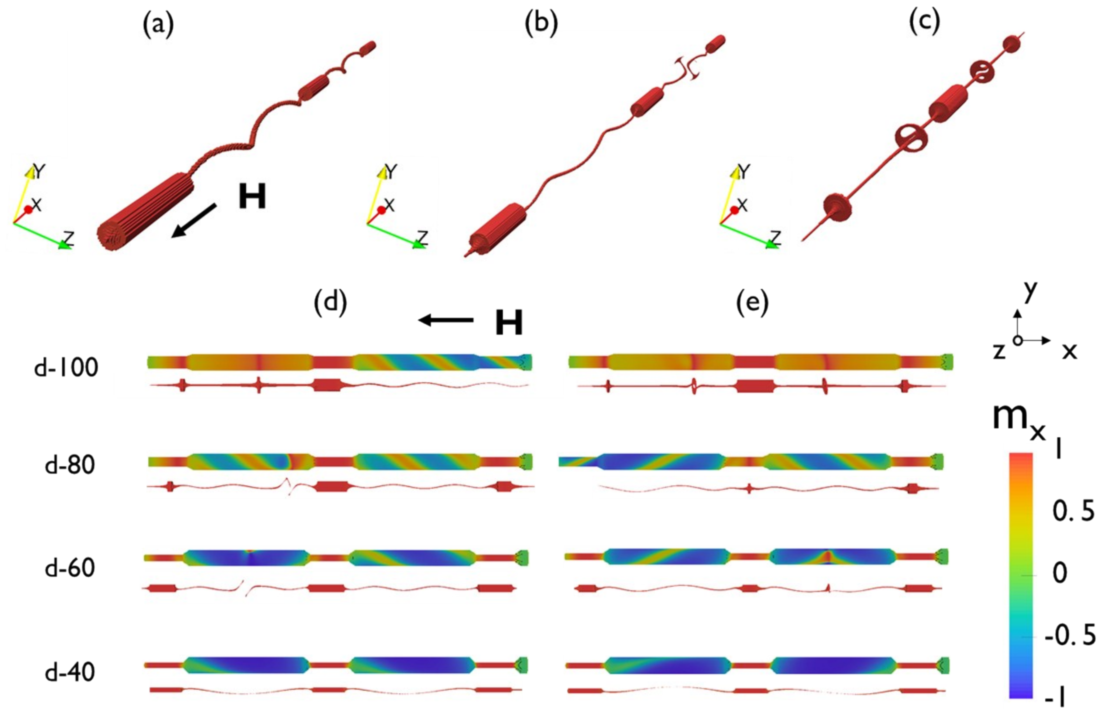

Figure SI4. *(a) Locus of m_x>0.97 in the nanowire with minor diameter 40 nm of distribution No. 2. (b) and (c) locus of m_x>0.97 in the nanowires with minor diameters 60 and 100 nm of distribution No.3. (d-e) From top to bottom, the longitudinal component of magnetization on the surface, and the locus of m_x>0.97 for each minor diameter of the nanowires of distribution No. 1*

Fig. SI4(d-e) show that the information of the inner part and the surface magnetization in a nanowire are correlated. Thus, measuring the longitudinal magnetization over the surface of the nanowire can give an idea about the magnetization inside. Summarizing, the following information form the inner part is encoded on the surface: First the presence of vortices/skyrmion tubes by a color magnetization gradient. If those tubes have opposite chiralities, the position where they meet can be inferred on the surface as an abrupt area where the magnetization is not reversed as a result of the vortex core displacement to the shell as is seen for diameters 80 and 60 nm from SI4(d) and 60 nm in SI4(e). Furthermore, the presence of a corkscrew structure is characterized by a twisted pattern of two opposite magnetization values on the surface and presents the same pitch as the inner helix. The chirality of the helix is also defined by the twisting direction. On the other hand, the transverse component of magnetization leads to a direct measurement of the chiralities of the vortices as shown in Fig SI3. In the case of 100 nm for SI4(d) helix also propagates inside the minor information. The latter provides useful information for analyzing XMCD-PEEM experimental data from the surface and the inner parts.

The characteristics of the core of the skyrmion tube have been studied at the fixed position in Fig 4a) along one line joining the nanowire center and the core of each skyrmion for each wire as shown in Fig 4 (b) and Fig SI5(a-b). The rotated angle of the core along the length is arbitrary. The longitudinal magnetization component along that line shows that the core of the skyrmion tube is magnetized along the saturation field direction (Fig. SI5(c-f)). The core width is reduced for narrow minor diameters and displaced form the center of the nanowire. The core width and displacement values are independent of the distribution with an eventual exception ascribed to the particular disorder differences.

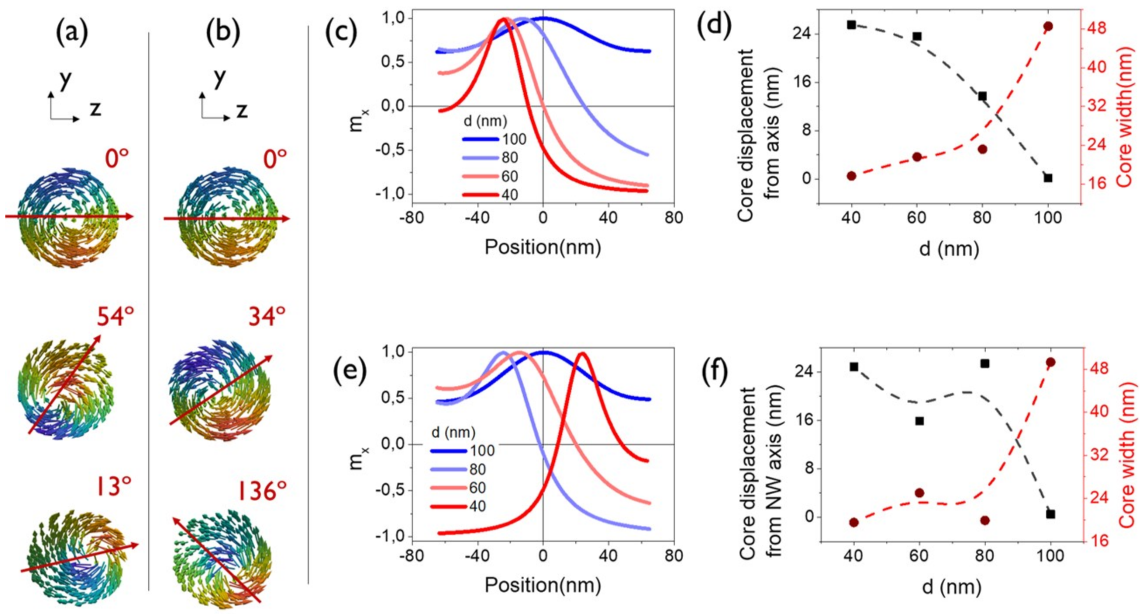

__Figure SI5.__ (a-b) Cross sections of the magnetization at the marked position in Fig 4(a) for nanowires with minor diameters 100, 80 and 40 nm (top to bottom) of distributions No. 2 and 3 respectively. Red arrows join the nanowire and the vortex/skyrmion centers for each cross *section. (c) and (e) Longitudinal component of the magnetization along the red arrows for the nanowires of disorder distributions No.2 and 3, respectively. (d) and (f) Core width and displacement from the nanowire axis as a function of the minor diameter for disorder distributions No. 2 and 3.*

The longitudinal magnetization components along the nanowire axis have been investigated for each distribution and diameter and confirm the non-periodic pitch of the helix in Fig. 3(c) and Fig. SI6(a-f). The presence of the corkscrew is determined by a large drop of the longitudinal magnetization component which has a "valley" -like shape when the initial vortices have the same chirality Fig. SI6(b-c, e-f) and presents a peak when they have opposite chiralities. The partial demagnetization of the minor segments is characterized by a step at each end of the catenary curve. For the nanowire with d=100nm of the disorder distribution 2, the vortex is deformed by the penetration inside of the minor diameter and there is a large shift of half catenary to lower values. The other magnetization components show information about the helical curling of the skyrmion tube. Despite the lack of periodicity of the helical structure, a quasiperiodic behavior is observed in the cases of vortices with same chirality in the modulations (Fig. SI6 (a-c, e, f)) which are particularly clear in Fig. SI6 (c, f) and Fig. 3(c): The local maxima of the oscillations of y and z magnetization components in the first modulation of Fig. 3(c) are separated by 308, 368 and again 308 nm, while in the second modulation by 294, 351 and 274 nm.

The complexity and the rich diversity of situations, begin a consequence of the particular disorder distribution of each nanowire, motivates further studies on the influence of the chiralities patterns in modulated nanowires for the future advanced technological applications.

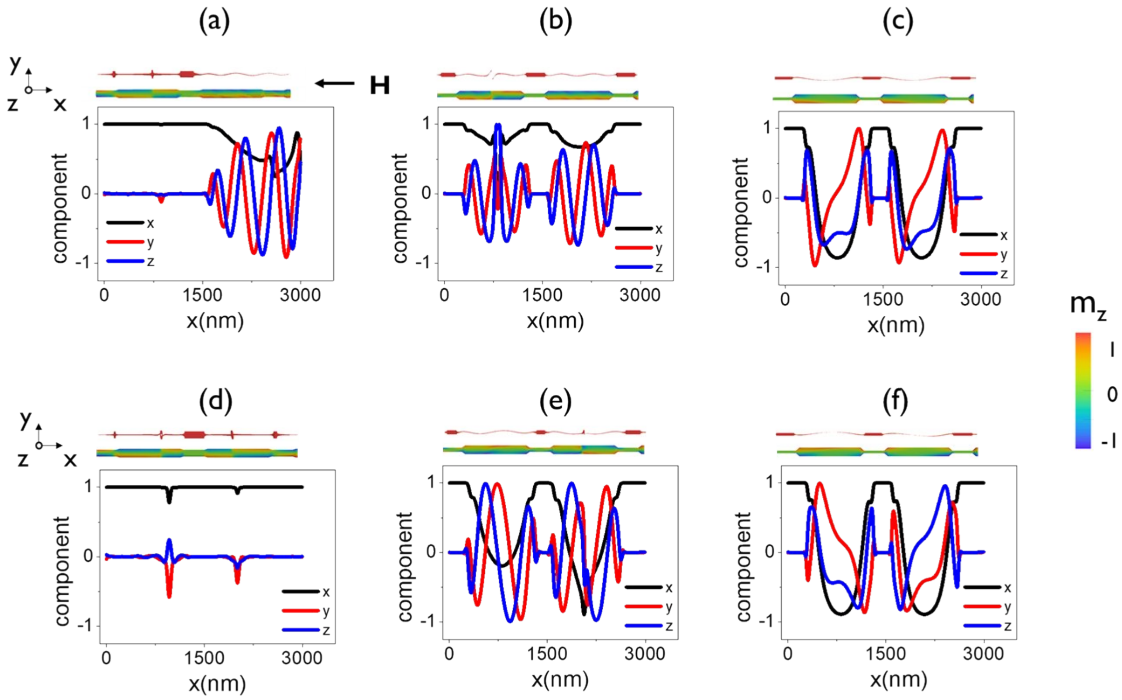

Figure SI6. *(a) and (b) Longitudinal magnetization components along the nanowire in nanowires with minor diameters d=100, 60 and 40 nm for disorder distributions No. 2 and 3, respectively. In each graph the geometry of the nanowire (bottom) and the locus of magnetization with* m_x*> 0.95 (top) are shown.*